

# Adaptive-Scale Filtering and Feature Detection Using Range Data

Clark F. Olson, *Member, IEEE*

**Abstract**—In edge and corner detection applications, it is typical to examine a single scale without knowing which scale is appropriate for each location in the image. However, many images contain a wide variation in the distance to the scene pixels and, thus, features of the same size can appear at greatly differing scales in the image. We present a method where the scale of the filtering and feature detection is varied locally according to the distance to the scene pixel, which we estimate through stereoscopy. The features that are detected are, thus, at the same scale in the world, rather than at the same scale in the image. This method has been implemented efficiently by filtering the image at a discrete set of scales and performing interpolation to estimate the response at the correct scale for each pixel. The application of this technique to an ordnance recognition problem has resulted in a considerable improvement in performance.

**Index Terms**—Filtering, edge detection, feature detection, stereo, smoothing, scale-space.

## 1 INTRODUCTION

IMAGE filtering and feature detection have been intensely studied subjects in computer vision and image processing. The selection of an appropriate filter size or scale for these processes is a problem that has received less attention. It is well-known that using a single fixed scale over the entire image produces undesirable results, since edge phenomena occur at a multitude of scales. To alleviate this problem, techniques have been developed that examine the entire space of scales [1], [2], [3], [4], or that adaptively select a scale based on local image properties [5], [6], [7], [8]. However, the optimal method for combining the information in the scale-space is unclear and scale selection methods that base their decisions on image properties, rather than the true scale at which the phenomena occur, can be confused by perspective effects.

In many applications, it is desirable to detect image phenomena that are at the same scale in the world, which we call the *true scale*, rather than at the same scale in the image or by selecting a scale based on local image properties. Consider, for example, an image containing a textured surface in the foreground and an object of interest further from the camera. Techniques based on local image properties consider the textured surface at the scale it appears in the image, where an irrelevant feature can appear significant, owing to perspective effects. If a method (such as stereoscopy) is available to determine the distance of the scene locations from the camera, we can safely smooth these phenomena, while preserving the significant edges. Furthermore, if we seek objects of known size, the filtering and feature detection processes can be tuned to

detect objects at the appropriate scale, regardless of the distance from the camera.

A motivating example is shown in Fig. 1. This image was collected at a live-fire test range near Nellis Air Force Base and contains two instances of live ordnance (one in the lower left, one in the upper right). In this case, the image was smoothed using a Gaussian filter with a constant scale ( $\sigma = 2.0$  pixels) prior to differentiation and edge detection. It can be observed in the edge map that the edges of the bomb at close range are rough and there is considerable clutter in the foreground. However, when the scale of smoothing is increased, the edges of the ordnance in the background are no longer sharp and the shape is distorted by the large size of the filter. We wish to be able to smooth the image and perform edge detection such that the edges of both instances of ordnance are well-behaved and there is little clutter in the edge map.

In addition to its value for scale selection, range data is also useful for determining edge salience with respect to the scene characteristics. For example, edge salience measures such as the length and straightness of the edge have been used [9]. However, the values these measures take are highly dependent on the distance of the edge from the camera. The range data can be used to normalize these measures with respect to the edge depth and it is, thus, possible to determine edge salience with respect to the true scale rather than the image scale.

The filtering techniques that we describe are general and can be applied to most edge and feature detection methods. We have implemented these techniques using a variation of the Canny operator [10] to perform edge detection and a variation of the Förstner and Gülch operator [11] to perform feature detection. A mapping function between the distance to the pixel and the image scale is first determined. We next filter the image at a discrete set of scales. The response for each pixel at the appropriate scale is then interpolated from the discrete set of filter responses (similar to ideas of steerable filters [12] or deformable kernels [13]). These

• The author is with the Jet Propulsion Laboratory, California Institute of Technology, 4800 Oak Grove Dr., Pasadena, CA 91109.  
E-mail: Clark.Olson@jpl.nasa.gov.

Manuscript received 13 Apr. 1999; revised 13 Oct. 1999; accepted 6 June 2000.

Recommended for acceptance by H. Christensen.

For information on obtaining reprints of this article, please send e-mail to: tpami@computer.org, and reference IEEECS Log Number 109596.

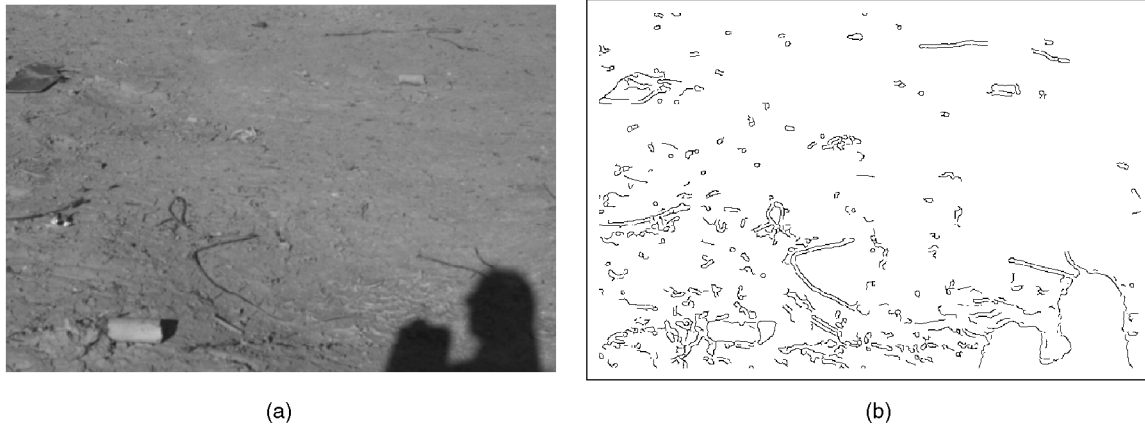


Fig. 1. Motivating example: (a) Original image. (b) Edges detection after Gaussian smoothing with  $\sigma = 2.0$  pixels.

responses are normalized, since the overall response to a general filter (e.g., a Gaussian derivative) is a function of the scale of the filter. Feature detection can then proceed according to the preferred operator.

## 2 PREVIOUS WORK

Since edges (and other features) appear at a wide variety of scales in an image, the concept of an image scale-space has been introduced [1], [4]. The scale-space can be defined as:

$$S(x, y, \sigma) = I(x, y) * g(x, y, \sigma) = \int_{-\infty}^{\infty} \int_{-\infty}^{\infty} I(u, v) \frac{1}{\sqrt{2\pi}\sigma} e^{-\frac{(x-u)^2 + (y-v)^2}{2\sigma^2}} dudv.$$

While many researchers have noted the need to examine a variety of scales in the image, the means by which the scale-space is used is not straightforward. One method that has been investigated by Bergholm [14] is to track edges through the scale-space in a coarse-to-fine manner. The edges are detected at a coarse scale and progressively refined through the examination of smaller scales. Alternatively, Lu and Jain [3] have devised a complex system of rules for reasoning about edges in the scale-space, including six rules governing the progression of scales examined. When the scale of the edge is unknown, they recommend starting at a maximum scale  $\sigma_1$  and decreasing the scale parameter by one pixel at each iteration.

Several methods of selecting a single local scale for each image pixel have also been proposed. Jeong and Kim [6] select the local scales through the minimization of an energy functional over the scale-space using a regularization approach. The functional includes terms that encourage a large scale in uniform intensity areas, a small scale where intensities change significantly and a smoothly varying scale over the image. Morrone et al. [8] suggest that the local scale should be a monotonically decreasing function of the gradient magnitude. They argue that this results in good localization through the use of a small scale when the contrast is high and good sensitivity using a large scale with the contrast is low. Lindeberg [7] notes that edge detection procedures seek to find maxima in the gradient magnitude in the spatial variables and that this principal can also be applied to the scale variable. He, thus, seeks the edge

position in the scale-space where gradient magnitude is maximized.

Elder and Zucker [5] select the "minimum reliable scale," which in their definition is the minimum scale at which the response level can be considered statistically reliable given the noise, edge amplitude, and image blur. This concept is used by Liang and Wang [15] to regulate an anisotropic diffusion process such that time at which the diffusion ends is computed for each pixel according to the minimum reliable scale given by a local noise estimate. Marimont and Rubner [16] also consider a minimum reliable scale, which they compute according to a statistical confidence measure.

Unlike these methods, we select the local scale of examination based on an estimate of the true scale, rather than trying to determine an appropriate scale through examination of the image. Our method is, thus, likely to yield better results when the real world scale is the important one. As an alternative to selecting a single scale, our techniques can be used to complement scale-space techniques [4]. In this case, the range data can be used to transform the scale-space such that each scale plane is level with respect to the true scale rather than the image scale.

## 3 DEPTH ACQUISITION

While any method that can associate range values with image pixels can be used with our adaptive filtering method, we use stereoscopy to compute dense range maps of the scene. The techniques that we use to compute the stereo range data have been described elsewhere [17], [18]. We briefly summarize this method here.

An off-line step, where the stereo camera rig is calibrated, is first performed. We use a perspective camera model [19] that has been extended to include radial lens distortion [20]. The remainder of the method is performed online.

At run time, each image is first warped to remove the lens distortion and the images are rectified so that the corresponding scanlines yield corresponding epipolar lines in the image. The disparity between the left and right images is measured for each pixel by minimizing the sum-of-squared-difference (SSD) measure of windows around the pixel in the Laplacian of the image. Subpixel

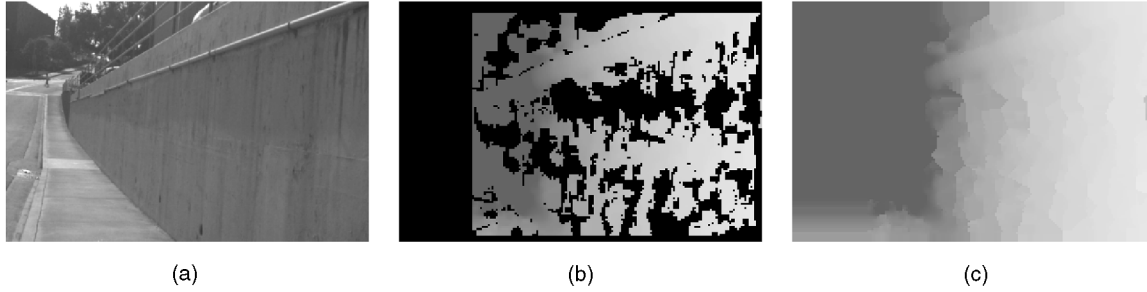


Fig. 2. Range data extracted from a stereo pair: (a) Left image of a stereo pair, (b) distance from the camera mapped into gray values (black pixels indicate no valid range data), and (c) distances after filling pixels with no range data.

disparity estimates are computed using parabolic interpolation on the SSD values neighboring the minimum. Outliers are removed through consistency checking and smoothing is performed over a  $3 \times 3$  window to reduce noise. Finally, the coordinates of each pixel are computed using triangulation.

Note that not every pixel is assigned a range with this method. There are a number of factors that result in various pixels not being assigned a range, including occlusion, window effects, finite disparity limits, low texture, and outliers. Despite this problem, we must have a range estimate at each pixel in the image in order to estimate the scale that should be used for smoothing at that pixel. To resolve this issue, we propagate the range values from neighboring pixels using a fast method for performing nearest-neighbor search.

Fig. 2 shows an example of the range data computed using these techniques. In this case, we fail to get range data at the left edge of the image, since this is the left image of a stereo pair and there are significant areas over the rest of the image where the range data is discarded as unreliable. These values are filled with estimates using the nearest-neighbor propagation techniques.

#### 4 FILTERING WITH VARIABLE SCALE

We perform variable scale filtering using the range data to select the appropriate scale at each pixel. The first step is to specify a mapping between the range data and the scale at which the smoothing should be performed. We map the range data into scales using:

$$\sigma(x, y) = \frac{K}{R(x, y)},$$

where  $R(x, y)$  is the range computed at the image pixel  $(x, y)$ ,  $\sigma(x, y)$  is the scale to be used at  $(x, y)$ , and  $K$  is a predetermined constant.

The constant,  $K$ , in this function can be determined using several methods. One possibility is to modify an automatic scale selection method (see, for example, [21]) to examine the image scale normalized by the depth values. A second possibility is to not limit ourselves to a single scale, but to consider the scale-space, with the scale-space warped such that the scale levels correspond to the true scale rather than the image scale. We use a third alternative. Since our primary application for these techniques is in detecting

objects of known size, we select  $K$  using the known size of the objects.

In order to smooth the image before the application of the feature detection methods, we should convolve the image with a Gaussian filter. However, since we vary the scale at each pixel, the responses that we desire are governed by:

$$S(x, y) = \sum_{i=-W}^W \sum_{j=-W}^W I(x+i, y+j) \frac{1}{\sigma(x, y)\sqrt{2\pi}} e^{-\frac{i^2+j^2}{2\sigma(x, y)^2}},$$

where  $I(x, y)$  is the image brightness at  $(x, y)$  and  $2W + 1$  is the filter size.

Unfortunately, it is time consuming to compute this function over an image, since there is no efficient implementation for the exact computation of the function. We approximate this function by convolving the image with a discrete set of Gaussian filters of various scales and interpolating the result at the appropriate scale for each pixel. This method for approximating a continuum of parameterized filters is similar to the techniques of steerable filters [12] and deformable kernels [13]. We have chosen parabolic interpolation rather than the linear combinations of the deformable kernels technique for simplicity and ease of implementation.

Since the range of scales that we are concerned with may be very large and Koenderink has shown that a logarithmic sampling of the scale space is stable and in accordance with the principle that no scale should be preferred above others [1], we work in the  $\log_2 \sigma$  domain. We have found that using discrete scales related by factors of two ( $\sigma_n = 2^n \sigma_0$ ) is both convenient and effective.

The result of smoothing at each pixel with a filter of scale  $\sigma(x, y)$  can be estimated through parabolic interpolation using the response of the discrete filter that is closest to the desired scale,  $F_{\sigma_k}(x, y)$ , and its two neighbors,  $F_{\sigma_{k-1}}(x, y)$  and  $F_{\sigma_{k+1}}(x, y)$ . In determining an equation that yields the appropriate response, it is useful to perform a coordinate transform such that  $z = \log_2 \frac{\sigma(x, y)}{\sigma_k}$ . For  $\sigma_{k-1} = \frac{1}{2}\sigma_k = \frac{1}{4}\sigma_{k+1}$ , this yields  $z_{k-1} = -1$ ,  $z_k = 0$ , and  $z_{k+1} = 1$ . With this transformation, it is simple to show that the interpolated result given by:

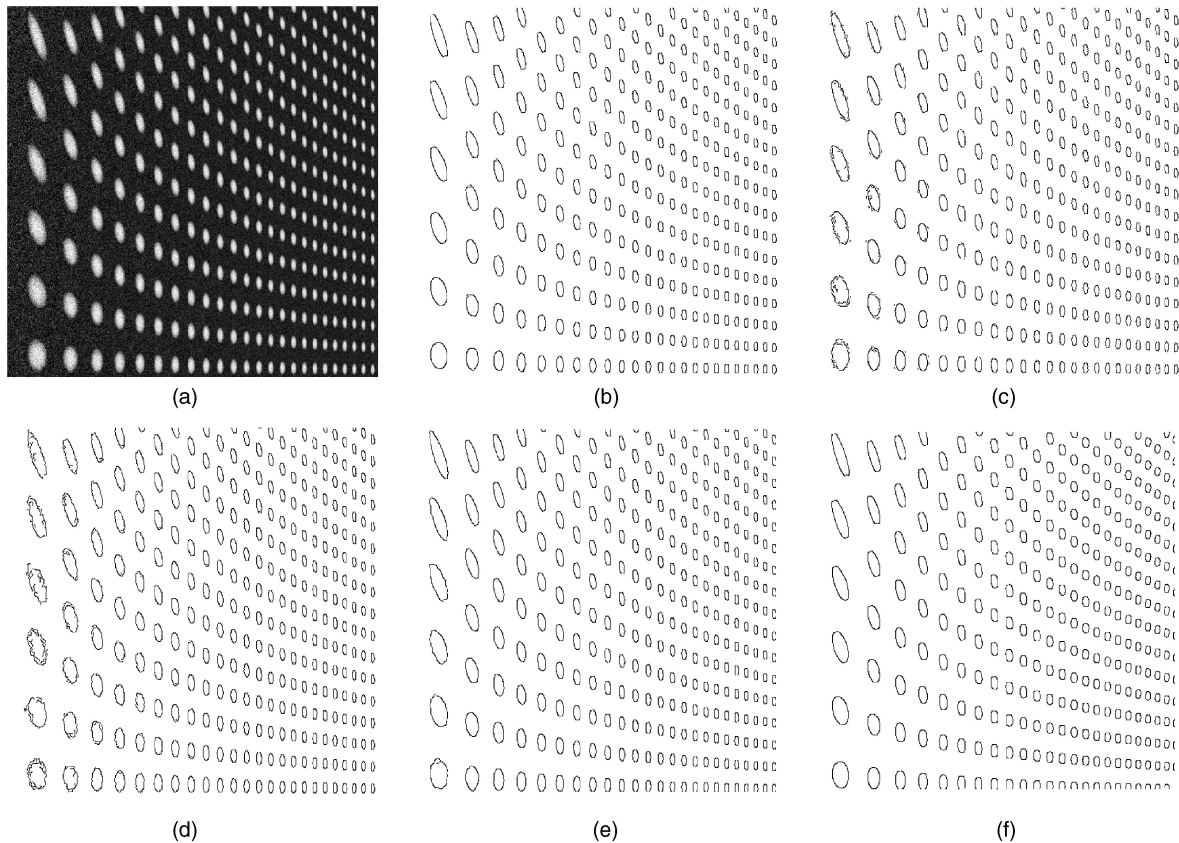


Fig. 3. Example applied to a synthetic image: (a) Original image, (b) edges detected with our method, (c) edges detected with Lindeberg's method, (d) edges detected with  $\sigma = 1.0$  pixels, (e) edges detected with  $\sigma = 2.0$  pixels, and (f) edges detected with  $\sigma = 4.0$  pixels.

$$F(x, y) \approx az^2 + bz + c$$

$$a = \frac{1}{2}(F_{\sigma_{k-1}}(x, y) - 2F_{\sigma_k}(x, y) + F_{\sigma_{k+1}}(x, y))$$

$$b = \frac{1}{2}(F_{\sigma_{k+1}}(x, y) - F_{\sigma_{k-1}}(x, y))$$

$$c = F_{\sigma_k}(x, y)$$

$$z = \log_2 \frac{\sigma(x, y)}{\sigma_k}$$

## 5 EDGE DETECTION

In our application of these techniques to edge detection, we use Canny's edge detection method [10] following the variable scale smoothing described above. This technique computes the image gradients over the image in the  $x$ - and  $y$ -directions in order to determine the orientation and magnitude of the gradient at each pixel. Note, however, that if the gradient magnitudes are to be comparable, we must normalize them. This can be easily recognized by observing that the response of a step edge to a Gaussian derivative filter varies with the scale of the filter. A Gaussian derivative aligned with a step edge yields a response proportional to  $\frac{1}{\sigma}$ . The gradient magnitudes will, thus, be stronger in the image regions that are smoothed at smaller scales if we do not normalize them. To correct this problem, we normalize the gradient magnitude at each pixel by multiplying by  $\sigma(x, y)$ . Finally, nonmaxima suppression is performed and the edges are detected using

hysteresis thresholding. We determine the hysteresis thresholds adaptively through examination of the histogram of gradient magnitudes.

Fig. 3 shows the application of these techniques to a synthetic image containing a warped plane of dots. Noise was added with a standard deviation that was inversely proportional to the range in order to simulate small-scale image texture that has increasing perceptual salience with decreasing range. For this example, it can be clearly seen that each of the edge maps detected with constant-scale smoothing is suboptimal (Fig. 3d, Fig. 3e, and Fig. 3f). When the scale is small, the noise in the image causes poor edge detection for the closer dots. When the scale is large, the shape of the smaller dots is distorted due to the large size of the smoothing operator. When variable-scale smoothing guided by range information is used, accurate edge maps are obtained at both large and small ranges. In addition, we used the ideas of Lindeberg [7] to choose a scale adaptively without using range data. This method selects the scale that maximizes the normalized gradient response. We approximated this measurement through parabolic interpolation of the same scales used by the range-guided smoothing. The adaptive-scale smoothing and edge detection method performed the best in this experiment.

Figs. 4 and 5 give examples of edge detection with and without stereo-guided scale selection on a pair of real images. The original images are  $750 \times 500$  pixels and can be found in Figs. 1 and 2. In these examples, the edges were detected at three scales ( $\sigma = 1.0, 2.0, 4.0$ ) without the help of

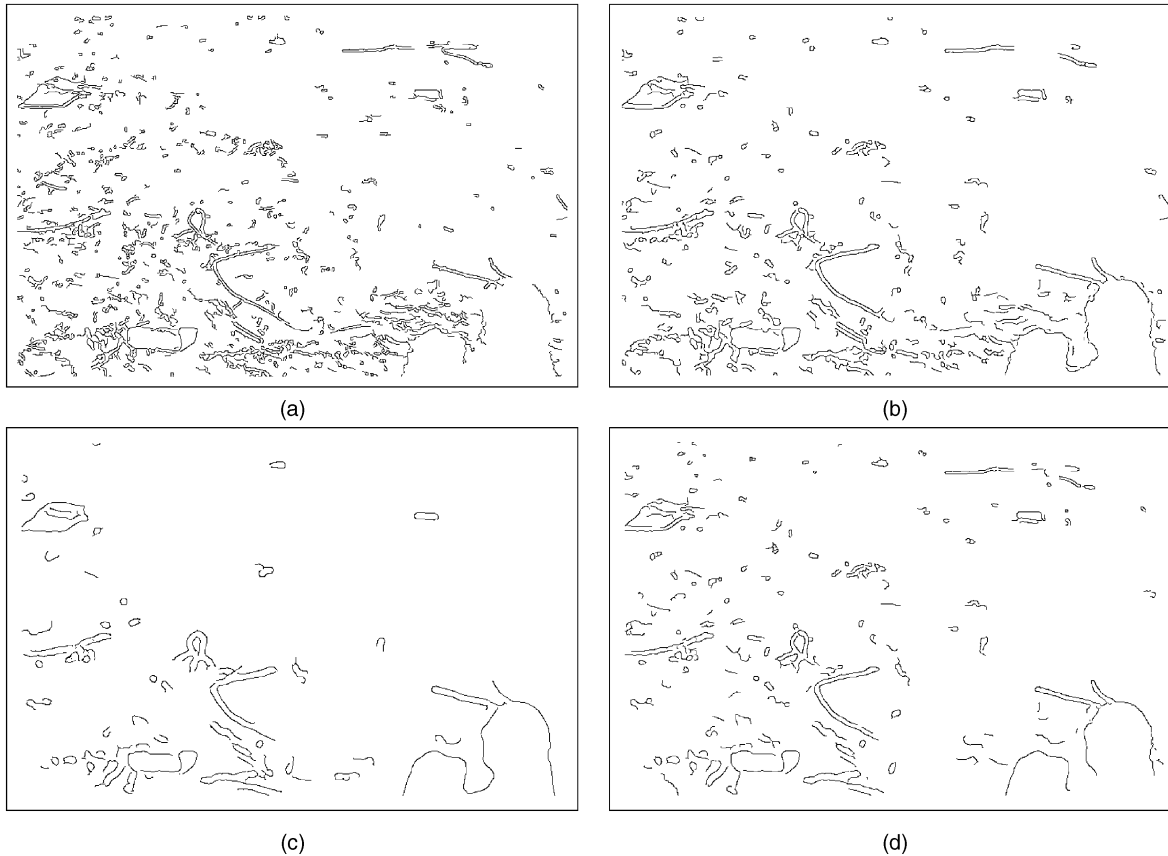


Fig. 4. Edge detection results for the image in Fig. 1: (a) Edges detected with  $\sigma = 1.0$ , (b) edges detected with  $\sigma = 2.0$ , (c) edges detected with  $\sigma = 4.0$ , and (d) edges detected with stereo-guided scale selection.

scale selection. Also given is the result with scale selection, where the response at each pixel was interpolated from the same three scales.

It can be seen that when a small scale ( $\sigma = 1.0$ ) is used, many of the edges, due to phenomena close to the camera, are rough and a number of extraneous edges are detected due to the small scale, even though there is little image texture. However, when the scale is increased, we lose the details at the further phenomena (see, for example, the trees in the background and the end of the railing in Fig. 5). On the other hand, when the scale is selected adaptively using the range data, we have good performance at both close and far edge phenomena.

## 6 EDGE SALIENCE EVALUATION

In addition to its use in performing edge detection, range data is also helpful in determining edge salience. Shorter edges that are detected at a larger distance are more likely to correspond to salient world edges than edges at close range that appear to be long due to perspective effects. We have primarily examined the summed gradient magnitude over the length of the edge and the local straightness of the edge as salience criteria, although many other salience measures could be used [9].

Consider, for example, a saliency measure where the gradient magnitude is summed along the length of the edge. The range data can be used to weight the gradient magnitude by the true edge length rather than the image

edge length.<sup>1</sup> Alternatively, we could sum the ranges to the pixels (normalized appropriately for the field-of-view and edge direction) to estimate the length of the edge in the world coordinates.

As a second example, we may consider the local straightness of the edges at each of their edge pixels by examining the difference in the gradient direction at neighboring edge pixels along the edge. However, we would not expect identical edge phenomena appearing at different ranges to yield the same differences in the gradient direction between the neighboring edge pixels. Edges closer to the camera will appear to be straighter, since the local gradient differences will be smaller. To allow for this effect, the differences in gradient direction can be weighted by the range to the edge.

## 7 FEATURE DETECTION

We have also applied these techniques to feature detection. In this case, we have used the method of Förstner and Gülch [11] subsequent to the Gaussian smoothing. Since this operator also uses the image derivatives to determine whether a feature should be detected, we must normalize the gradients as was done for the edge detection. For each

1. For nonfrontal scenery, the orientation of the edge also affects the edge length. This effect can be accounted for if we estimate the three-dimensional orientation of the edge.

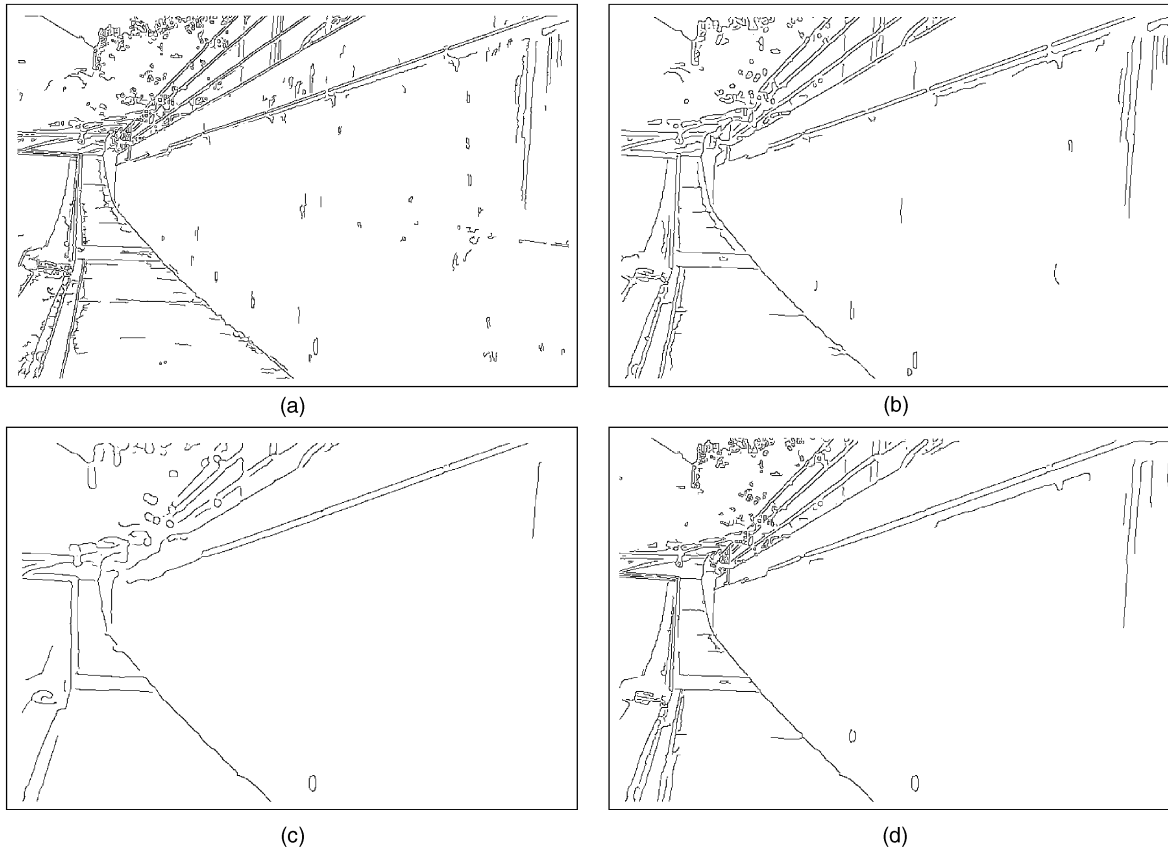


Fig. 5. Edge detection results for the image in Fig. 2: (a) Edges detected with  $\sigma = 1.0$ , (b) edges detected with  $\sigma = 2.0$ , (c) edges detected with  $\sigma = 4.0$ , and (d) edges detected with stereo-guided scale selection.

pixel, we then compute the circularity of the confidence ellipse  $q$  and the precision  $w$ :

$$q = \frac{4 \cdot \det(N)}{\text{trace}(N)^2}$$

$$w = \frac{2 \cdot \det(N)}{\text{trace}(N)}$$

$$N = \begin{bmatrix} \left(\frac{\delta I}{\delta x}\right)^2 & \frac{\delta I}{\delta x} \cdot \frac{\delta I}{\delta y} \\ \frac{\delta I}{\delta x} \cdot \frac{\delta I}{\delta y} & \left(\frac{\delta I}{\delta y}\right)^2 \end{bmatrix}.$$

The circularity  $q$  is between zero and one. We desire values closer to one, since this indicates gradients in multiple directions, rather than a single straight edge. A large value for  $w$  indicates the presence of strong gradients and measures the precision of the feature localization. We, thus, select, as corners, those positions that are local maxima and have  $w$  and  $q$  above some threshold value.

Fig. 6 shows an example of the application of these techniques to an image of Mars from the Pathfinder mission. It can be observed that when corners are detected with adaptive scale selection, fewer features are detected in the foreground, since they are less relevant. On the other hand, more features are detected further from the camera, where they are more relevant, but appear smaller due to the perspective transformation.

## 8 APPLICATION RESULTS

Our target application for these techniques is to recognize surface-lying ordnance in military test ranges using a stereo system mounted on an unmanned ground vehicle for the purpose of autonomous remediation. One method to evaluate the edge detection techniques is by the performance of this application when using the stereo-guided smoothing and edge detection versus the performance when it is not used. We have tested the techniques on a set of 48 gray-scale images consisting of barren terrain with an inert piece of ordnance present at various distances and orientations (see Fig. 7).

In this experiment, we tested three scales individually ( $\sigma = 0.8, 1.6, 3.2$ ) and the result with stereo-guided scale selection using the same three scales to interpolate from. After edge detection was performed, an algorithm to detect the ordnance using geometric cues was used to find candidate ordnance positions [22]. We also considered the combination of all of the candidates found at the three discrete scales (with duplicates removed).

Table 1 summarizes the results of this experiment. When the variable-scale smoothing and edge detection was performed, we achieved 40 correct recognitions out of the 48 cases. The eight failures occurred due to cases where the ordnance was at a significant distance from the camera and at an orientation nearly aligned with the camera axis (the worst case). In addition, 18 false positives were detected in

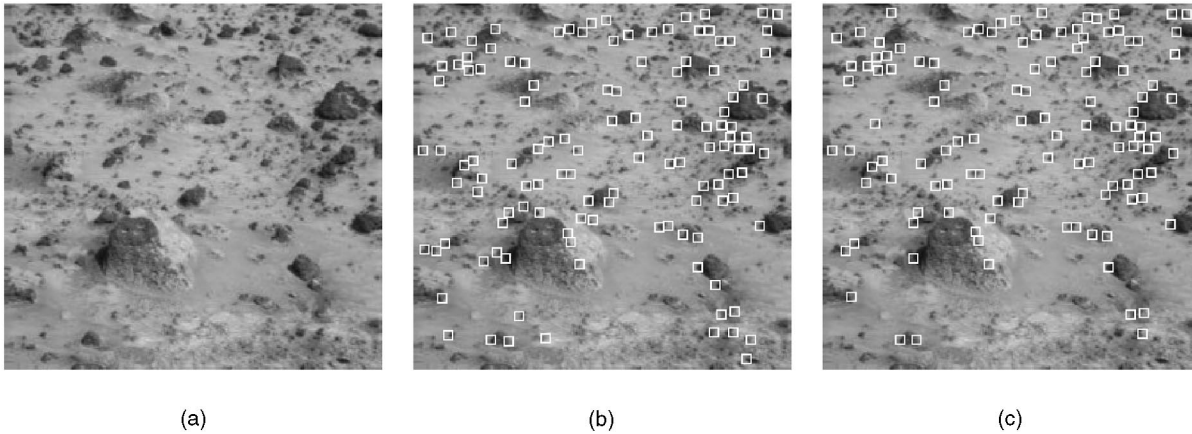


Fig. 6. Feature extraction using adaptive scale selection: (a) Original image, (b) corners detected with  $\sigma = 2.0$ , and (c) corners detected with adaptive scale selection.

the images. Fig. 7 shows two examples, one of which contains a false positive.

For each individual scale that was examined, we had more cases where the ordnance was missed than with stereo-guided scale selection and, in two of them, we also found more false positives. While the largest constant scale that was examined ( $\sigma = 4.0$  pixels) resulted in four fewer false positives, the detection performance was significantly degraded, since five additional ordnance instances were missed. When all of the candidates from the three scales were combined, there was one less false negative, but in this case the number of false positives rose sharply to 45.

Overall, the use of the stereo-guided scale selection techniques resulted in performance that was significantly superior to any of the individual scales or the combination of the scales.

## 9 DISCUSSION

In the application of these techniques, there are some practical issues that should be considered, since the techniques may not be appropriate for all situations. A potential drawback to our method is that it relies on first obtaining a dense depth map of the scene. Some methods for estimating depth do not generate dense values. Even in methods that estimate dense values, areas of low texture can cause measurements to be significantly in error. In the stereo method that we use [17], measurements are pruned if they are suspected to be inaccurate. This can be observed in Fig. 2b, where the black areas correspond to pruned data. We use nearest-neighbor propagation techniques to fill the

unknown values. This is adequate in many cases. However, some depth estimation methods may produce measurements that are too sparse to be generate good estimates. In this case, the performance of our method will be degraded. In general, errors in the range estimates cause a suboptimal filter scale to be used. However, in this method it is critical only to use a scale near the optimal value at each location. Small deviations in the estimated scale do not cause large changes in the derived edge map. Note also that areas of low texture, where depth estimates are likely to be in error, are areas in which we will not detect any edges or other features. Areas that contain features are likely to yield accurate depth estimation, since correlation-based matching techniques work well in these areas.

Another issue of concern in some applications is the existence of occlusion boundaries where the depth map is not smooth. In this case, the filter will span multiple depths at these locations and will, therefore, be inappropriate for a portion of the image to which they are applied. A related issue is whether it is appropriate to look for a single “true scale” for any location in the image, when events occur over the space of scales. In some applications, using the image depth to select a single scale for each image location may be inappropriate. However, there are many useful applications where this simplifying assumption yields excellent results and requires less computation than considering the full space of scales. An example can be seen in the ordnance recognition application we discussed in Section 8. Where there are depth discontinuities, our experience is that the stereo estimate usually corresponds to the surface with greater texture. If we are to choose a single depth for these locations, this estimate is a reasonable (perhaps the best) one to choose.

Lindeberg and Gårding [23] have described a related technique to perform smoothing adaptively. They use local image measurements to determine the appropriate shape of the filter in order to reduce distortions that occur in the estimation of 3D shape. This technique was applied to improving both shape-from-texture and shape-from-disparity by applying the adaptive smoothing techniques prior to estimating the shape of the surfaces. They further suggest an approach where the adaptive smoothing is guided by the interimage deformations for use in shape-from-disparity.

TABLE 1  
Results in Ordnance Recognition Application

Scale	False negatives	False positives
1.0	12	28
2.0	11	28
4.0	13	14
all	7	45
variable	8	18

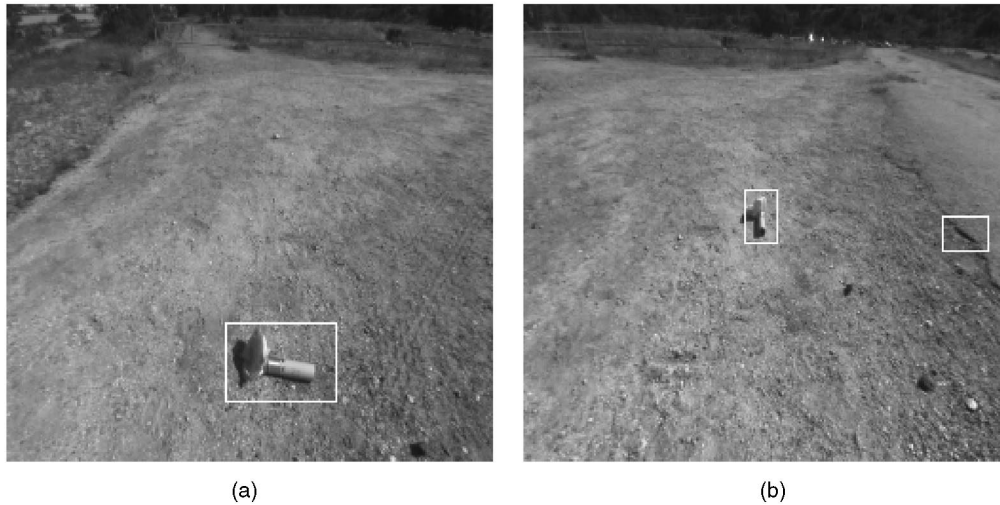


Fig 7. Ordnance recognition examples: (a) Correct detection at close range. (b) Correct detection at medium range and a false positive.

This method would adapt the shape of the filters such that the filters applied to the left and right images backproject to the same patch in the world (up to a first-order approximation). Our approach, while not attempting to achieve this same backprojection, uses a similar idea, where range estimates derived from the stereo pair are used to guide the smoothing process. This method could be adapted to use local shape estimates from the image to guide the shape of the smoothing filter in a manner similar to that suggested by Lindeberg and Gårding.

## 10 SUMMARY

We have described techniques that perform filtering and feature detection (edges and corners) adaptively using range data to select the scale at each pixel. This allows processing of the image to be performed with respect to the true scale of objects rather than the scale observed in the image. We have also used the range data for evaluating the saliency of edges with respect to the true scale. These techniques have been implemented by convolving the image with Gaussian derivatives at a discrete set of scales. The correct response at each image pixel is estimated through parabolic interpolation of the known responses and normalization is performed so that the results are comparable across the image. Improved results were obtained after the variable-scale filtering using both Canny's edge detector [10] and the feature detection method of Förstner and Gülch [11]. In addition, the application of this method to the problem of detecting unexploded ordnance in test ranges has resulted in a considerable improvement in performance.

## ACKNOWLEDGMENTS

The research described in this paper was carried out by the Jet Propulsion Laboratory, California Institute of Technology, and was sponsored by the Air Force Research Laboratory at Tyndall Air Force Base, Panama City, Florida, through an agreement with the National Aeronautics and Space Administration. Reference herein to any specific commercial product does not constitute or imply its endorsement by the United States Government, the Jet

Propulsion Laboratory, or the California Institute of Technology. A preliminary version of this work appeared in the 1998 IEEE Computer Society Conference on Computer Vision and Pattern Recognition [24].

## REFERENCES

- [1] J.J. Koenderink, "The Structure of Images," *Biological Cybernetics*, vol. 50, pp. 363–370, 1984.
- [2] T. Lindeberg, "Detecting Salient Blob-Like Image Structures and Their Scales with a Scalespace Primal Sketch: A Method for Focus-of-Attention," *Int'l J. Computer Vision*, vol. 11, no. 3, pp. 283–318, 1993.
- [3] Y. Lu and R.C. Jain, "Reasoning About Edges in Scale Space," *IEEE Trans. Pattern Analysis and Machine Intelligence*, vol. 14, no. 4, pp. 450–468, Apr. 1992.
- [4] A.P. Witkin, "Scale-Space Filtering," *Proc. Int'l Joint Conf. Artificial Intelligence*, vol. 2, pp. 1,019–1,022, 1983.
- [5] J.H. Elder and S.W. Zucker, "Local Scale Control for Edge Detection and Blur Estimation," *IEEE Trans. Pattern Analysis and Machine Intelligence*, vol. 20, no. 7, pp. 699–716, July 1998.
- [6] H. Jeong and C.I. Kim, "Adaptive Determination of Filter Scales for Edge Detection," *IEEE Trans. Pattern Analysis and Machine Intelligence*, vol. 14, no. 5, pp. 579–585, May 1992.
- [7] T. Lindeberg, "Edge Detection and Ridge Detection with Automatic Scale Selection," *Proc. IEEE Conf. Computer Vision and Pattern Recognition*, pp. 465–470, 1996.
- [8] M.C. Morrone, A. Navangione, and D. Burr, "An Adaptive Approach to Scale Selection for Line and Edge Detection," *Pattern Recognition Letters*, vol. 16, pp. 667–677, 1995.
- [9] P.L. Rosin, "Edges: Saliency Measures and Automatic Thresholding," *Machine Vision and Applications*, vol. 9, pp. 139–159, 1997.
- [10] J. Canny, "A Computational Approach to Edge Detection," *IEEE Trans. Pattern Analysis and Machine Intelligence*, vol. 8, no. 6, pp. 679–697, Nov. 1986.
- [11] W. Förstner and E. Gülch, "A Fast Operator for Detection and Precise Locations of Distinct Points, Corners, and Centres of Circular Features," *Proc. Intercommission Conf. Fast Processing of Photogrammetric Data*, pp. 281–305, 1987.
- [12] W.T. Freeman and E.H. Adelson, "The Design and Use of Steerable Filters," *IEEE Trans. Pattern Analysis and Machine Intelligence*, vol. 13, no. 9, pp. 891–906, Sept. 1991.
- [13] P. Perona, "Deformable Kernels for Early Vision," *IEEE Trans. Pattern Analysis and Machine Intelligence*, vol. 17, no. 5, pp. 488–499, May 1995.
- [14] F. Bergholm, "Edge Focusing," *IEEE Trans. Pattern Analysis and Machine Intelligence*, vol. 9, no. 6, pp. 726–741, Nov. 1987.
- [15] P. Liang and Y.F. Wang, "Local Scale Controlled Anisotropic Diffusion with Local Noise Estimate for Image Smoothing and Edge Detection," *Proc. Int'l Conf. Computer Vision*, pp. 193–200, 1998.

- [16] D.H. Marimont and Y. Rubner, "A Probabilistic Framework for Edge Detection and Scale Selection," *Proc. Int'l Conf. Computer Vision*, pp. 207–214, 1998.
- [17] L. Matthies, "Stereo Vision for Planetary Rovers: Stochastic Modeling to Near Real-Time Implementation," *Int'l J. Computer Vision*, vol. 8, no. 1, pp. 71–91, July 1992.
- [18] L. Matthies, A. Kelly, T. Litwin, and G. Tharp, "Obstacle Detection for Unmanned Ground Vehicles: A Progress Report," *Proc. Int'l Symp. Robotics Research*, pp. 475–486, 1996.
- [19] Y. Yakimovsky and R. Cunningham, "A System for Extracting Three-Dimensional Measurements from a Stereo Pair of TV Cameras," *Computer Vision, Graphics, and Image Processing*, vol. 7, pp. 195–210, 1978.
- [20] D.B. Gennery, "Camera Calibration Including Lens Distortion," JPL internal report D-8580, Jet Propulsion Laboratory, California Institute of Technology, 1991.
- [21] E.R. Hancock and J. Kittler, "Adaptive Estimation of Hysteresis Thresholds," *Proc. IEEE Conf. Computer Vision and Pattern Recognition*, pp. 196–201, 1991.
- [22] C.F. Olson and L.H. Matthies, "Visual Ordnance Recognition for Clearing Test Ranges," *Proc. (SPIE '98) Detection and Remediation Technologies for Mines and Mine-Like Targets III*, vol. 3,392, pp. 122–133, 1998.
- [23] T. Lindeberg and J. Gårding, "Shape-Adaptive Smoothing in Estimation of 3D Shape Cues from Affine Deformations of Local 2D Brightness Structure," *Image and Vision Computing*, vol. 15, pp. 415–434, 1997.
- [24] C.F. Olson, "Variable-Scale Smoothing and Edge Detection Guided by Stereoscopia," *Proc. IEEE Conf. Computer Vision and Pattern Recognition*, pp. 80–85, 1998.



**Clark F. Olson** (S'92-M'94) received the BS degree in computer engineering and the MS degree in electrical engineering from the University of Washington in 1989 and 1990, respectively. He received the PhD degree in computer science from the University of California, Berkeley, in 1994. After spending two years as a post-doctoral researcher at Cornell University, he was employed by the Jet Propulsion Laboratory, California Institute of Technology, Pasadena, CA, where he is currently a member of the Machine Vision group. His research interests include computer vision and mobile robotics.